Variability of fire carbon emissions in Equatorial Asia and its non-linear sensitivity to El Niño

Yi Yin[1*], Philippe Ciais[1], Frederic Chevallier[1], Guido R. van der Werf[2], Thierry Fanin[2], Gregoire Broquet[1], Hartmut Boesch[3,4], Anne Cozic[1], Didier Hauglustaine[1], Sophie Szopa[1], Yilong Wang[1]

[1] Laboratoire des Sciences du Climat et de l'Environnement, CEA-CNRS-UVSQ, UMR8212, Gif-sur-Yvette, France.

[2] Earth and Climate Cluster, Department of Earth Sciences, Faculty of Earth and Life Sciences, VU University, De Boelelaan 1085, 1081HV, Amsterdam, The Netherlands.

[3] Earth Observation Science, Department of Physics and Astronomy, University of Leicester, Leicester, UK.

[4] NERC National Centre for Earth Observation, UK.

* Corresponding author: Yi Yin (yi.yin@lsce.ipsl.fr)

Key Points:

- 0.5±0.17 (1σ) Pg carbon emitted from the Equatorial Asia peat fires in 2015 as constrained by atmospheric inversion.
- Fire carbon emissions increase exponentially with cumulative water deficit, possible to forecast it with a lead time of 2 months.
- We infer a total fire carbon loss ranging from 12 to 25 Pg by 2100 in the coming decades based on future climate projections from CMIP5.

Post-print of: Yin, Y. et al. "Variability of fire carbon emissions in Equatorial Asia and its non-linear sensitivity to El Niño" in Geophysical research letters, vol. 43, issue 19 (Oct. 2016), p. 10.472-10.479. The final version is available at DOI 10.1002/2016GL070971

Abstract

The large peatland carbon stocks in the land use change-affected areas of Equatorial Asia are vulnerable to fire. Combining satellite observations of active fire, burned area, and atmospheric concentrations of combustion tracers with a Bayesian inversion, we estimated the amount and variability of fire carbon emissions in Equatorial Asia over the period 1997-2015. Emissions in 2015 were of 0.51±0.17 Pg carbon – less than half of the emissions from the previous 1997 extreme El Niño, explained by a less acute water deficit. Fire severity could be empirically hindcasted from the cumulative water deficit with a lead time of 1 to 2 months. Based on future climate projections and an exponential empirical relationship found between fire carbon emissions and water deficit, we infer a total fire carbon loss ranging from 12 to 25 Pg by 2100 in the coming decades, a significant positive feedback to future climate warming.

1 Introduction

Equatorial Asia (EQAS) tropical peatlands accumulated over thousands of years hold about 70 Pg of organic carbon (C) [*Page et al.*, 2011], a large pool comparable to the forest biomass of the entire Amazon [*Saatchi et al.*, 2011]. Fires are typically lit by humans as a management tool in EQAS, but the burning often goes out of control during dry years, especially in areas where peatland drainage for agriculture and palm plantation has lowered the water table [*van der Werf et al.*, 2008]. Abnormally large fires occur during El Niño droughts, causing negative health, ecological, and economic impacts [*Field et al.*, 2009; *Marlier et al.*, 2015]. An iconic example is the extreme Indonesian fire event associated with the 1997 El Niño, which was estimated to release 0.8–2.6 Pg C to the atmosphere [*Page et al.*, 2002]. In the dry season 2015, the El Niño index reached again an extremely high value comparable to that of the 1997/98 [*NOAA*, 2016]. Various media reported a significant positive fire anomaly in Indonesia in September and October 2015. Yet, a robust estimation of the fire carbon loss is challenging given the large uncertainties in the detection of peat fires due to the low temperature anomaly of smoldering and underground burning, and the blocking of heavy smoke [*Tansey et al.*, 2008]. Considerable uncertainties also lie in the estimation of burning depth and fuel consumption [*Page et al.*, 2002; *van der Werf et al.*, 2008, 2010; *Ballhorn et al.*, 2009; *Konecny et al.*, 2015].

Atmospheric observations of carbon-fuel combustion tracers, i.e. carbon monoxide (CO), carbon dioxide (CO_2), methane (CH_4), and formaldehyde (CH_2O), are thus valuable to provide additional top-down constraints to the regional fire carbon emissions using inverse modeling. Among these tracers, CO is particularly useful in tracking biomass burning emissions, because it shows significant regional enhancement over pyrogenic sources, its average lifetime of 2 months allows atmospheric transport models to track the fire pollution plumes, and it is one of the best observed tracers with its spatial-temporal variations well quantified over recent 15 years from space [*Yin et al.*, 2015]. Here, using a sophisticated multi-tracer 4-D Var Bayesian inversion system, this study aims at (1) quantifying the variability of fire emissions in the EQAS over the last 19 years, (2) documenting how fire carbon

emissions respond to climate variability covering records of two extreme El Nino events, and (3) estimating future fire carbon emissions in the coming century.

2 Materials and Methods

In this study, we analyzed the fire dynamics in EQAS based on bottom-up satellite-derived ground fire data and atmospheric carbon combustion tracer concentrations since the early 2000s. Using a global multi-tracer (CH_4–CH_2O–CO) atmospheric inversion, we calculated a top-down estimate of the EQAS fire carbon emissions for the period of 2002-2015 and extended it back to 1997 based on the strong correlation between bottom-up and top-down estimates. Further, we analyzed the correlation between fire emissions and climate over the last 19 years, and estimated future fire carbon emissions by 2100 based on climate projections from the model ensembles of Coupled Model Intercomparison Project Phase5 (CMIP5). Three types of observational datasets are used: (1) ground fire features, (2) atmospheric tracer concentrations, and (3) climate proxies (**Table S1**). In addition, future climate projections from CMIP5 are analyzed (**Table S3**).

2.1 Ground fire feature analysis

MODIS daily active fire products – MOD14A1 from Terra and MYD14A1 from Aqua with local pass time of 10:30 and 13:30 [*Giglio et al.*, 2006] are analyzed. The lowest detection confidence level of active fires was chosen because smoldering fires could be classified as lower confidence due to their lower burning temperatures. The ratios of peat fires to total fire counts are calculated based on the high-resolution peat distribution map [*Wetland International*, 2015] for the three main islands, Sumatra, Borneo, and West Papua, where over 90% of the EQAS peats are distributed (**Fig. S1**). We also analyzed two burned area products – MCD45A1 [*Roy et al.*, 2008] and MCD64A1 [*Giglio et al.*, 2013]. These datasets are complemented by the Global Fire Emissions Database (GFED4), which provides not only a

bottom-up estimate of burned area but also fire type and emissions of various tracers from 1997 to 2015 [*Randerson et al.*, 2015]. Last, emission estimates from Global Fire Assimilation System (GFAS) based on fire radiative power are also analyzed, covering the recent period from 2003 to 2015 [*Kaiser et al.*, 2012].

2.2 Atmospheric inversion

Fire CO emissions in this study are quantified for the period from 2002 to 2015 using a global multi-tracer (CH_4–CH_2O–CO) atmospheric Bayesian inversion system as detailed in *Yin et al.*, [2015 and references therein]. Satellite total column retrievals of CO from the Measurements Of Pollution In The Troposphere (MOPITT) (available for a full year since 2002) [*Deeter et al.*, 2014] and CH_2O from the Ozone Monitoring Instrument (OMI) (available since 2004) [*González Abad et al.*, 2015] are assimilated jointly with surface in situ measurements of CH_4 and methyl-chloroform (MCF). Very limited surface stations are located within or around the EQAS region, providing only background constraints to the regional budgets. The results of CH_4 and MCF from surface stations are thus not addressed in this paper.

The inversion optimizes prior CO emissions compiled from biomass burning emissions from GFED4 (or GFAS for sensitivity tests; **Table S2**), fossil fuel emission inventory from MACCity [*Lamarque et al.*, 2010], and ocean biogenic emissions from model climatology (See details in [*Yin et al.*, 2015]). Fire attribution of the optimized total CO emissions is empirically estimated based on the inter-annual variation (IAV) of the posterior fluxes and the relative fire contribution according to the prior information (details in Supplementary Information). Fire total carbon (TC) emissions are then estimated from fire CO emissions using the ratio of emission factors between TC and CO. Three burning types are differentiated – peat, deforestation, and agriculture, with average TC:CO ratios of 2.81, 5.28, and 4.7 respectively, following GFED [*van der Werf et al.*, 2010]. A Monte Carlo approach is used to estimate the uncertainty of the TC emissions, accounting for the propagation of errors in the CO inversion as described by [*Chevallier et al.*, 2007] and in the fire emission partitioning and emission factor ratios (arbitrarily set

as 30%) (**Text S2**). Then, fire carbon emissions of the pre-MOPITT period (1997-2001) are estimated using the linear regression between the annual bottom-up and top-down estimates of the period from 2002 onwards.

2.3 Future emission estimates

Correlation between the monthly fire TC emissions and climate variability over the major emission regions over the last 19 years are analyzed, including precipitation, temperature, evapotranspiration, and multivariate ENSO index (MEI). Future climate projections of precipitation and evapotranspiration from 24 models in the CMIP5 ensembles [*Taylor et al.*, 2012] and from seven models that has been bias corrected for the climate forcing variables (precipitation and surface air temperature) [*Hempel et al.*, 2013] are used to estimate future cumulative fire TC emissions (see model list in **Table S3**). The empirical relationship found between the fire TC emissions and accumulative water deficit are applied to estimate the amplitude of future fire carbon emissions (**Text S3**).

3 Results and Discussion

3.1 Anomaly of surface fire counts and burned area

In September-October 2015, active fire counts [*Giglio et al.*, 2006] reached the highest values observed by the Moderate Resolution Imaging Spectroradiometer (MODIS) instruments since 2000 (**Fig. 1a**). The 2015 fire counts are 2.7 and 2.4 times the decadal average as observed in the morning and afternoon, respectively (**Fig. 1a**). Positive fire anomalies in 2015 occurred mainly in southeast Sumatra, southern Borneo, and West Papua, where most EQAS peatlands locate [*Wetland International*, 2015] (**Fig. 2a-b)**. The 2015 fire anomaly is also embedded in a progressive increase of peat burning from 2007 onwards (**Fig. S2**). Over peat-rich ecosystems, fire counts remained similar between the morning and afternoon, whereas in other ecosystems, more fires occurred in the afternoon (**Fig. S2**). The fire

persistence index, defined as the ratio between continuously detected daily fires and the total fire counts over a year, shows a similar inter-annual variation (IAV) as the peat fire proportion [*van der Werf et al.*, 2008] and the ratio of morning-to-afternoon fire counts, confirming that peat fires are more persistent and continue to burn for days once ignited.

The MODIS burned areas, derived from surface reflectance change, also show positive fire anomalies in 2015 (**Fig. 1b**). The 2015 burned areas estimated by the two products listed above, MCD45 [*Roy et al.*, 2008] and MCD64 [*Giglio et al.*, 2013], are 2.7 and 2.1 times the decadal average, respectively. The GFED4 burned area, which is based on MCD64 and extends back to 1997 from other satellites, further shows that the 2015 burned area was 30% lower than that of 1997. The two burned area datasets have a similar IAV, but MCD64 finds systematically 5-10 times more burned area than MCD45, in line with previous studies suggesting that MCD45 is low-biased due to a greater cloud and aerosol contamination [*Roy et al.*, 2008]. The differences in the magnitude and spatial distribution of fire anomalies between the two burned area datasets illustrate the large uncertainties in identifying EQAS fire emissions with bottom-up fire observation alone (**Fig. 2c-d**). The uncertainty in peat burning depth could further complicate bottom-up fire emission estimates from burned area [*Ballhorn et al.*, 2009; *Konecny et al.*, 2015]. Moreover, cloud cover significantly decreased after 2013, when the El Niño state started to build up (**Fig. 1c**), which increases the probability of fire detection by satellite and may bias the interpretation of fire trends based on burned area and active fire. Thus, a top-down approach is useful to quantify the amount and variability of regional fire carbon emissions from atmospheric tracer signals.

3.2 Anomaly of atmospheric tracer concentrations

Abnormally high column concentrations of CO were observed by MOPITT over the EQAS region in 2015 (**Fig. 2e**). The average regional enhancement of CO was ~63 ppb (parts-per-billion, 10^{-9}), i.e. 66% higher than the decadal average dry season level (Jun. to Oct.) (**Fig. 1e**). The peaks in CO column concentrations echoes with high active fire counts. The OMI satellite retrievals of CH_2O – whose

sources are direct surface emission and oxidation of volatile organic compounds (VOCs) – also showed a positive anomaly of ~100 ppt (parts-per-trillion, 10^{-12}) in 2015, 34% higher than the mean decadal dry season level (**Fig. 1d**). The peaks in both CO and CH_2O concentrations provide evidence for abnormally high fire emissions during El Niño years (2002, 2006, 2009 and 2015), as shown in **Fig. 1.**

The total column concentrations of CO_2 (X_{CO2}) as observed by the Greenhouse Gases Observing Satellite (GOSAT) [*Cogan et al.*, 2012] and Orbiting Carbon Observatory (OCO-2) [*Crisp et al.*, 2012] also show significant positive enhancements in 2015 compared to the detrended mean seasonal cycle (2009-2015) (**Fig. 3;** See **Fig. S3** for comparison with other regions). The magnitude of the regional X_{CO2} enhancement is around 1.2 ppm (parts-per-million, 10^{-6}) in September and reached 1.6 ppm in November 2015. A direct attribution of this X_{CO2} anomaly to EQAS fire emission is complicated because of the additional and uncertain contribution from terrestrial and oceanic CO_2 fluxes induced by the El Niño climate anomaly. Therefore, we chose to use measurements of CO to infer fire emissions, because CO is a more direct proxy tracer of fire carbon emissions and the time series of CO observations are longer than those of X_{CO2}.

3.3 Fire carbon emission and climate variability

We inferred the optimized CO emissions (posterior estimate) that best fit atmospheric CO (MOPITT) and CH_2O (OMI) satellite measurements using the inversion summarized in section 2.2 from 2002 to 2015. For the year 2015, the inversion shows lower CO emissions from Sumatra but higher emissions from Borneo compared to the prior (**Fig. S4**). The optimized EQAS CO emission in 2015 is 134±19 Tg (with 122 Tg CO attributed to fire emissions), accounting for 10.5% of the global CO emissions. The top-down estimates of the regional emissions show a similar IAV as the bottom-up fire datasets (GFED and GFAS) (**Fig. 4a**). We extended the TC emission estimates to the pre-MOPITT period using linear regression between the annual bottom-up (average of the three datasets shown in **Fig. 4a**) and top-down estimates of 2002 onwards as shown in **Fig. 4b** (R^2=0.92). The inversion approach gives an

emission of 0.51±0.17 Pg C in 2015, which is less than half of the emissions inferred during the 1997 El Niño (1.21±0.45 Pg C). Considering a 30% lower burned area of 2015 with regard to 1997, the greater decrease in fire carbon emissions indicates lower fuel combustion per area in 2015. The EQAS cumulative fire emission since 1997 is of 4±1.3 Pg C.

The water deficit in the dry season 2015 was less acute than in 1997 (-165 mm vs. -210 mm); the MEI in 2015 is also lower compared to 1997 (2.31 vs. 2.69). The rainfall anomaly also suggests a longer drought season and a larger rainfall deficit in 1997 compared to 2015, for the fire concentrated regions in southern Sumatra and Borneo as well as for the entire EQAS (**Fig. S5**). Monthly TC emissions are found to increase exponentially with cumulative water deficit (precipitation minus evapotranspiration) (**Fig. 5a**). Exponentially increasing TC emissions are also observed with decreasing cumulative precipitation or increasing ENSO index during the fire season (**Fig. S6a-b**). The best exponential fit is obtained using four-months cumulative water deficit preceding the fire season (Jun. to Oct.), suggesting that using the cumulative water deficit is more robust for TC emission estimates compared to using precipitation or ENSO index as predictors. Cumulative precipitation or water deficit preceding the fire season with a lead time of 1 to 2 months could also effectively forecast the amount of fire emissions (**Fig. S6c-d**), which may contribute to an early warning for EQAS peat fire management.

3.4 Future fire emission projection

The frequency of extreme El Niño events simulated by climate models is projected to nearly double in the coming decades [*Cai et al.*, 2014]. Climate models also indicate an increase in severe drought events in the EQAS region, with the potential to increase fire emissions [*Lestari et al.*, 2014]. Based on future climate model projections from CMIP5 and the empirical relationship found between fire TC emission and cumulative water deficit shown in **Fig. 5a**, we estimated a total cumulative peat fire carbon loss of 25±20 Pg C in EQAS by 2100 following the current climate warming trajectory (Representative Concentration Pathway RCP 8.5) [*Meinshausen et al.*, 2011] (13±9 Pg C in RCP 4.5)

(**Fig. 5b; Text S3**). The large uncertainty reflects the spread of climate model projections. Our simple method to estimate future emissions ignores exhaustion of peat stocks prone to burning and future changes in human drivers such as policies of fire management and peat conservation [*van der Werf et al.*, 2008; *Carlson et al.*, 2012; *Busch et al.*, 2015]. Nevertheless, it shows the magnitude of the peat carbon deposits that are at stake under future climate change.

4 Conclusions

Satellite observations of ground fire features and atmospheric pollutant concentrations provided us new insights into fire dynamics and fire associated carbon losses in the EQAS, where massive land use change due to agriculture and palm plantation are taking place over the carbon-rich peat soils in recent decades [*Carlson et al.*, 2012; *Margono et al.*, 2014]. The strong nonlinear relationship found between fire emissions and cumulative water deficit suggests a high future risk of peat carbon loss due to fire given that future climate projections indicate a two-fold increase in the frequency of extreme El Niño [*Cai et al.*, 2014]. In the absence of actions to limit peat burning, our results show that peat fire CO_2 emissions to the atmosphere will act as a positive feedback on climate change, whose magnitude is one-quarter of the permafrost feedback [*Schuur et al.*, 2015]. However, such process is not yet represented in current Earth system models. Offsetting this long-term carbon source will require stronger mitigation measures to keep climate warming below 2°C as stated in the UN Paris Climate Agreement.

Figure Captions

Fig. 1. Time series of monthly fire related proxies from 2000 to 2015. (a) Active fire counts derived from MODIS in the morning (MOD14) and the afternoon (MYD14); **(b)** Burned area estimated by two MODIS datasets (MCD45 and MCD64). A different scale is used for MCD45 – right-y-axis; **(c)** Cloud counts associated with MODIS active fires; **(d)** Atmospheric column concentration of CH_2O (X_{CH2O}) over EQAS from OMI; **(e)** Atmospheric column concentration of CO (X_{CO}) over EQAS from MOPITT. Grey shades in the background show the bimonthly multivariate ENSO index – the darker the color, the higher the value.

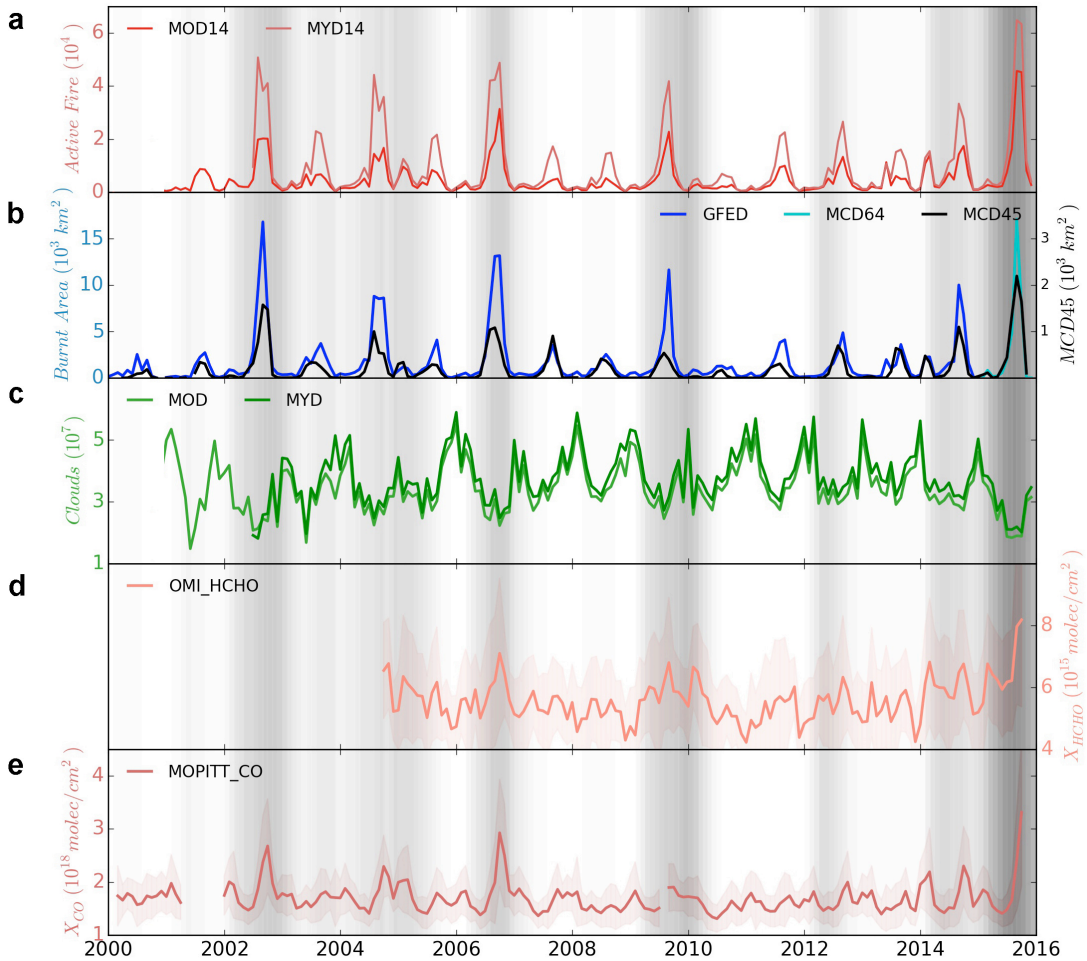

Fig. 2. Spatial distribution of fire anomaly in 2015. (a) Mean annual active fire counts from both the morning (MOD14) and the afternoon (MYD14); **(b)** Active fire anomaly; **(c)** Burned area anomaly in MCD45 compared to its multi-year average (2003-2015); **(d)** Burned area anomaly in MCD64 compared to its multi-year average (2003-2015); **(e)** MOPITT X_{CO} anomaly in October 2015 compared to its multi-year October average (2002-2015).

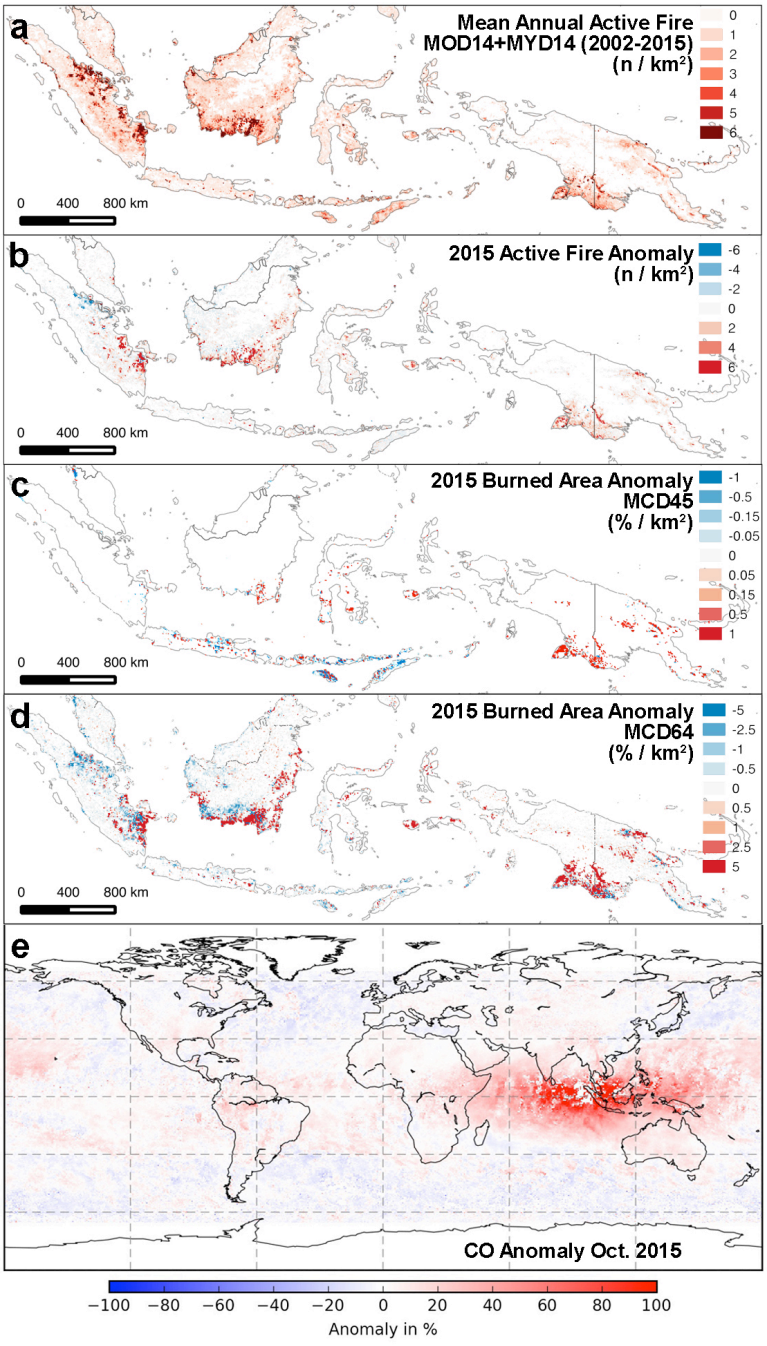

Fig. 3. The concentration of CO_2 total column (X_{CO2}) over EQAS observed by GOSAT and OCO-2. **(a)** Regional X_{CO2} concentration from April 2009 to Dec 2015; **(b)** the seasonal cycle of the detrended X_{CO2} for each year.

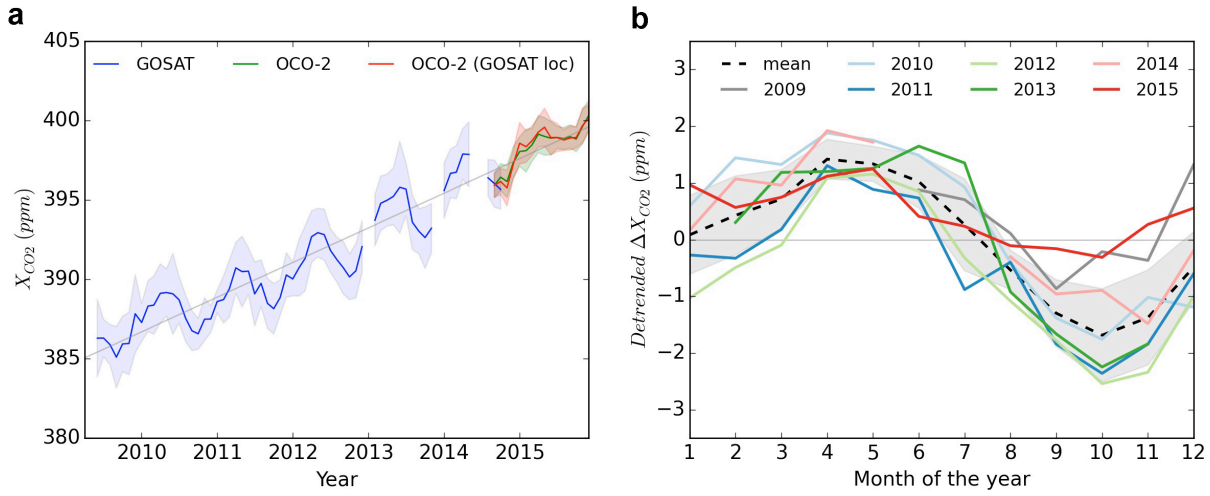

Fig. 4. Fire carbon emissions from EQAS. (a) Monthly TC emissions estimated by the bottom-up and top-down approaches. The dashed line shows the dynamics of multivariate ENSO index. **(b)** Scatter of the annual TC emissions obtained by the bottom-up and top-down approaches from 2002 to 2015. Shaded areas show 2-σ uncertainty ranges.

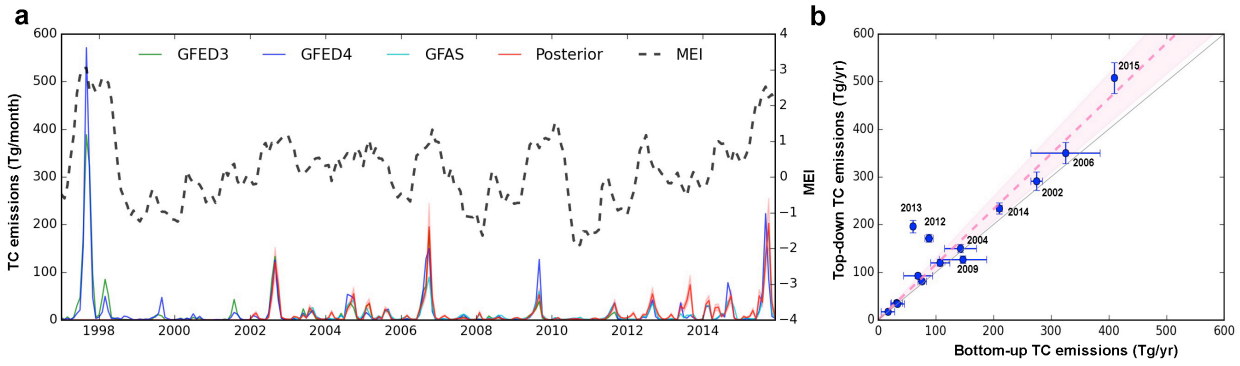

Fig. 5. (a) Monthly fire carbon emissions as a function of the cumulative water deficits of four months. **(b)** Future projections of fire carbon emissions based on future climate projections of seven bias-corrected CMIP5 models and the empirical relationship in (a). Solid lines represent the model median; shaded areas represent the range between 25th and 75th quantile of the model ensembles.

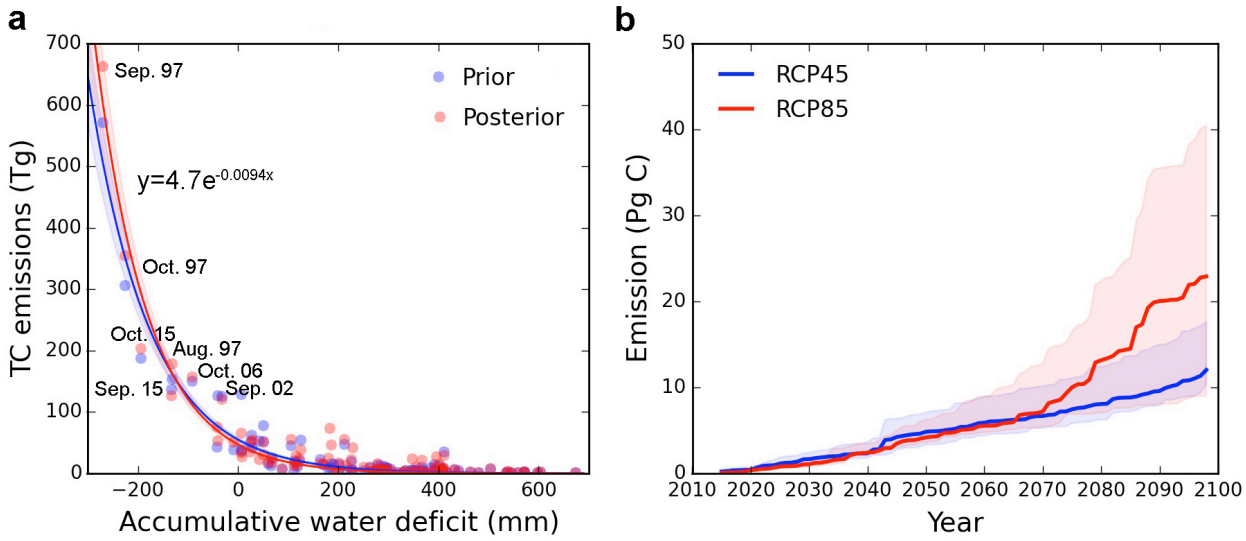

Acknowledgments and Data

Data to support this article can be obtained by contacting the corresponding author by email (yi.yin@lsce.ipsl.fr). This study is supported by the European Research Council Synergy grant ERC-2013-SyG 610028 (IMBALANCE-P). We acknowledge the following data providers: NCAR MOPITT for satellite CO retrievals, SAO OMI for CH_2O retrievals, Leicester GOSAT and JPL/MIT OCO-2 for CO_2 retrievals. We also wish to thank F. Marabelle and his team for computer support at LSCE.

References

Ballhorn, U., F. Siegert, M. Mason, and S. Limin (2009), Derivation of burn scar depths and estimation of carbon emissions with LIDAR in Indonesian peatlands., *Proc. Natl. Acad. Sci. U. S. A.*, *106*(50),

21213–8, doi:10.1073/pnas.0906457106.

Busch, J. et al. (2015), Reductions in emissions from deforestation from Indonesia's moratorium on new oil palm, timber, and logging concessions., *Proc. Natl. Acad. Sci. U. S. A.*, *112*(5), 1328–33, doi:10.1073/pnas.1412514112.

Cai, W. et al. (2014), Increasing frequency of extreme El Niño events due to greenhouse warming, *Nat. Clim. Chang.*, *4*(2), 111–116, doi:10.1038/nclimate2100.

Carlson, K. M., L. M. Curran, D. Ratnasari, A. M. Pittman, B. S. Soares-Filho, G. P. Asner, S. N. Trigg, D. A. Gaveau, D. Lawrence, and H. O. Rodrigues (2012), Committed carbon emissions, deforestation, and community land conversion from oil palm plantation expansion in West Kalimantan, Indonesia., *Proc. Natl. Acad. Sci. U. S. A.*, *109*(19), 7559–64, doi:10.1073/pnas.1200452109.

Chevallier, F., F.-M. Bréon, and P. J. Rayner (2007), Contribution of the Orbiting Carbon Observatory to the estimation of CO 2 sources and sinks: Theoretical study in a variational data assimilation framework, *J. Geophys. Res.*, *112*(D9), D09307, doi:10.1029/2006JD007375.

Cogan, A. J. et al. (2012), Atmospheric carbon dioxide retrieved from the Greenhouse gases Observing SATellite (GOSAT): Comparison with ground-based TCCON observations and GEOS-Chem model calculations, *J. Geophys. Res. Atmos.*, *117*(D21), doi:10.1029/2012JD018087.

Crisp, D. et al. (2012), The ACOS CO_2 retrieval algorithm – Part II: Global X_{CO2} data characterization, *Atmos. Meas. Tech.*, *5*(4), 687–707, doi:10.5194/amt-5-687-2012.

Deeter, M. N., S. Martínez-Alonso, D. P. Edwards, L. K. Emmons, J. C. Gille, H. M. Worden, C. Sweeney, J. V. Pittman, B. C. Daube, and S. C. Wofsy (2014), The MOPITT Version 6 product: algorithm enhancements and validation, *Atmos. Meas. Tech.*, *7*(11), 3623–3632, doi:10.5194/amt-7-3623-2014.

Field, R. D., G. R. van der Werf, and S. S. P. Shen (2009), Human amplification of drought-induced biomass burning in Indonesia since 1960, *Nat. Geosci.*, *2*(3), 185–188, doi:10.1038/ngeo443.

Giglio, L., I. Csiszar, and C. O. Justice (2006), Global distribution and seasonality of active fires as observed with the Terra and Aqua Moderate Resolution Imaging Spectroradiometer (MODIS) sensors, *J. Geophys. Res.*, *111*(G2), G02016, doi:10.1029/2005JG000142.

Giglio, L., J. T. Randerson, and G. R. van der Werf (2013), Analysis of daily, monthly, and annual burned area using the fourth-generation global fire emissions database (GFED4), *J. Geophys. Res. Biogeosciences*, *118*(1), 317–328, doi:10.1002/jgrg.20042.

González Abad, G., X. Liu, K. Chance, H. Wang, T. P. Kurosu, and R. Suleiman (2015), Updated Smithsonian Astrophysical Observatory Ozone Monitoring Instrument (SAO OMI) formaldehyde retrieval, *Atmos. Meas. Tech.*, *8*(1), 19–32, doi:10.5194/amt-8-19-2015.

Hempel, S., K. Frieler, L. Warszawski, J. Schewe, and F. Piontek (2013), A trend-preserving bias correction – the ISI-MIP approach, *Earth Syst. Dyn.*, *4*(2), 219–236, doi:10.5194/esd-4-219-2013.

Kaiser, J. W. et al. (2012), Biomass burning emissions estimated with a global fire assimilation system based on observed fire radiative power, *Biogeosciences*, *9*(1), 527–554, doi:10.5194/bg-9-527-2012.

Konecny, K., U. Ballhorn, P. Navratil, J. Jubanski, S. E. Page, K. Tansey, A. Hooijer, R. Vernimmen, and F. Siegert (2015), Variable carbon losses from recurrent fires in drained tropical peatlands., *Glob. Chang. Biol.*, doi:10.1111/gcb.13186.

Lamarque, J. F. et al. (2010), Historical (1850–2000) gridded anthropogenic and biomass burning emissions of reactive gases and aerosols: methodology and application, *Atmos. Chem. Phys.*, *10*(15), 7017–7039.

Lestari, R. K., M. Watanabe, Y. Imada, H. Shiogama, R. D. Field, T. Takemura, and M. Kimoto (2014), Increasing potential of biomass burning over Sumatra, Indonesia induced by anthropogenic tropical warming, *Environ. Res. Lett.*, *9*(10), 104010, doi:10.1088/1748-9326/9/10/104010.

Margono, B. A., P. V. Potapov, S. Turubanova, F. Stolle, and M. C. Hansen (2014), Primary forest cover loss in Indonesia over 2000–2012, *Nat. Clim. Chang.*, *4*(8), 730–735, doi:10.1038/nclimate2277.

Marlier, M. E., R. S. DeFries, P. S. Kim, D. L. A. Gaveau, S. N. Koplitz, D. J. Jacob, L. J. Mickley, B. A. Margono, and S. S. Myers (2015), Regional air quality impacts of future fire emissions in Sumatra and Kalimantan, *Environ. Res. Lett.*, *10*(5), 054010, doi:10.1088/1748-9326/10/5/054010.

Meinshausen, M. et al. (2011), The RCP greenhouse gas concentrations and their extensions from 1765 to 2300, *Clim. Change*, *109*(1-2), 213–241, doi:10.1007/s10584-011-0156-z.

NOAA (2016), Multivariate ENSO Index (MEI), Available from: http://www.esrl.noaa.gov/psd/enso/mei/

Page, S. E., F. Siegert, J. O. Rieley, H.-D. V Boehm, A. Jaya, and S. Limin (2002), The amount of carbon released from peat and forest fires in Indonesia during 1997., *Nature*, *420*(6911), 61–5, doi:10.1038/nature01131.

Page, S. E., J. O. Rieley, and C. J. Banks (2011), Global and regional importance of the tropical peatland carbon pool, *Glob. Chang. Biol.*, *17*(2), 798–818, doi:10.1111/j.1365-2486.2010.02279.x.

Randerson, J. T., G. R. van der Werf, L. Giglio, G. J. Collatz, and P. S. Kasibhatla (2015), Global Fire Emissions Database, Version 4, (GFEDv4), , doi:http://dx.doi.org/10.3334/ORNLDAAC/1293.

Roy, D. P., L. Boschetti, C. O. Justice, and J. Ju (2008), The collection 5 MODIS burned area product — Global evaluation by comparison with the MODIS active fire product, *Remote Sens. Environ.*, *112*(9), 3690–3707, doi:10.1016/j.rse.2008.05.013.

Saatchi, S. S. et al. (2011), Benchmark map of forest carbon stocks in tropical regions across three continents., *Proc. Natl. Acad. Sci. U. S. A.*, *108*(24), 9899–904, doi:10.1073/pnas.1019576108.

Schuur, E. A. G. et al. (2015), Climate change and the permafrost carbon feedback, *Nature*, *520*(7546), 171–9, doi:10.1038/nature14338.

Tansey, K., J. Beston, A. Hoscilo, S. E. Page, and C. U. Paredes Hernández (2008), Relationship between MODIS fire hot spot count and burned area in a degraded tropical peat swamp forest in Central Kalimantan, Indonesia, *J. Geophys. Res.*, *113*(D23), D23112, doi:10.1029/2008JD010717.

Taylor, K. E., R. J. Stouffer, and G. A. Meehl (2012), An Overview of CMIP5 and the Experiment Design, *Bull. Am. Meteorol. Soc.*, *93*(4), 485–498, doi:10.1175/BAMS-D-11-00094.1.

van der Werf, G. R. et al. (2008), Climate regulation of fire emissions and deforestation in equatorial Asia, *Proc. Natl. Acad. Sci. U. S. A.*, *105*(51), 20350–5, doi:10.1073/pnas.0803375105.

van der Werf, G. R., J. T. Randerson, L. Giglio, G. J. Collatz, M. Mu, P. S. Kasibhatla, D. C. Morton, R. S. DeFries, Y. Jin, and T. T. van Leeuwen (2010), Global fire emissions and the contribution of deforestation, savanna, forest, agricultural, and peat fires (1997–2009), *Atmos. Chem. Phys.*, *10*(23), 11707–11735.

Wetland International (2015), *Peat Atlas - Sumatra, Kalimantan, Papua*.

Yin, Y., F. Chevallier, P. Ciais, G. Broquet, A. Fortems-Cheiney, I. Pison, and M. Saunois (2015), Decadal trends in global CO emissions as seen by MOPITT, *Atmos. Chem. Phys.*, *15*(23), 13433–13451, doi:10.5194/acp-15-13433-2015.